Kinetic model of carbon nanotube production from carbon dioxide in a floating catalytic chemical vapour deposition reactor

Geoffrey S. Simate,[a] Kapil Moothi,[ab] M. Meyyappan,[c] Sunny E. Iyuke,*[ab] Sehliselo Ndlovu,[a] Rosemary Falcon[a] and Mike Heydenrych[d]

The production of carbon nanostructures, including carbon nanotubes (CNTs), by chemical vapour deposition (CVD) occurs by thermally induced decomposition of carbon-containing precursors. The decomposition of the feedstock leading to intermediate reaction products is an important step, but rarely incorporated in rate equations, since it is generally assumed that carbon diffusion through or over the catalyst nanoparticles is the rate-limiting step in the production of CNTs. Furthermore, there is no kinetic model to date for the production of CNTs from carbon dioxide. These aspects are addressed in this study with the aid of a series of experiments conducted in a floating catalytic CVD reactor in which the effects of reactor temperature, concentration and flow rate of CO_2 were investigated. A simple rate equation for the reductive adsorption of CO_2 onto the catalyst surface followed by carbon diffusion leading to the production of CNTs is proposed as follows: $d[CNT]/dt = K[CO_2]$, where K is proportional to the diffusion coefficient of carbon. The derived kinetic model is used to calculate the amount of CNTs for a given concentration of CO_2, and the experimentally measured data fits the simple rate equation very well at low carbon dioxide concentration.

Introduction

Carbon dioxide (CO_2) is the most prevalent greenhouse gas that traps heat and raises the global temperature. Interest in its use as a raw material in the synthetic chemical industry has increased over the past few decades[1–4] including the possibility of using CO_2 in the production of carbon nanotubes (CNTs).[5] Due to their interesting electronic properties and exceptional mechanical properties, CNTs have received much attention for application in electronics, high strength composites, chemical and biosensors, field emission devices, filters and membranes, catalyst support, water purification and numerous others.[6] Despite the large potential of using CNTs in various applications, the major problem is low production rate. Besides the arc discharge process, chemical vapor deposition (CVD) has been a popular technique for depositing CNTs on substrates as well as for bulk production.[6] The floating catalyst CVD (FC-CVD) method shows much promise for continuous, large-scale synthesis of high purity CNTs.[7] A modified version of this approach using swirled flow, known as swirled floating catalytic chemical vapour deposition (SFCCVD), has emerged recently[8] and this process has been successfully applied for the growth of multi-walled CNTs (MWCNTs) and single-walled CNTs (SWCNTs).[9,10] The SFCCVD method has been found to be more successful both in terms of operational practicality and CNT yield than the microwave or the fixed-bed catalytic CVD modes.[10–13] In the pursuit of large scale and continuous production of CNTs, kinetic studies of their formation have continued to be a subject of interest. However, unlike CNTs produced from other carbon sources,[14–17] there is a dearth of literature on the kinetic modelling of CNTs produced from CO_2. The present work is devoted to the development of a simple kinetic model for the production of CNTs using CO_2.

Materials and methods

The CNTs were produced by a method similar to that of Xu and Huang[18] using a 10% iron catalyst on calcium carbonate support. The choice of calcium carbonate was based on the good quality, high yield and high purity materials obtained from its use as a support.[19] The catalyst was prepared by a modified wet impregnation technique[20] by mixing a predetermined amount of iron nitrate and citric acid in approximately 1 : 1 molar ratio in deionized water. Ammonia solution was added in drops until a neutral pH was reached. A reddish brown solution with no precipitate was obtained after a period

[a]School of Chemical and Metallurgical Engineering, University of the Witwatersrand, P/Bag 3, Wits 2050, Johannesburg, South Africa. E-mail: sunny.iyuke@wits.ac.za
[b]DST/NRF Centre of Excellence in Strong Materials, P/Bag 3, Wits 2050, Johannesburg, South Africa
[c]Center for Nanotechnology, NASA Ames Research Center, Moffett Field, CA 94035, USA
[d]Department of Chemical Engineering, University of Pretoria, P/Bag X20, Hatfield 0028, South Africa

of six hours. A calculated amount of calcium carbonate was then stirred into this solution to form a dry slurry, which was then left to stand overnight. The resulting powder was calcined at 500 °C between 2 and 12 h in a muffle furnace to decompose the nitrates from the catalyst.[21]

Fig. 1 shows a SFCCVD reactor used to synthesize CNTs, which consists of a vertical quartz or silica plug-flow reactor inside a furnace. The upper end of the reactor is connected to a condenser that leads to two delivery cyclones where the CNTs are collected. Feed materials including carrier gases are uniformly mixed with the aid of a swirled coiled mixer to give optimum interaction. The flow of gases into the SFCCVD reactor is aided by a system of valves and rotameters.[22]

Approximately 10 g of the catalyst was placed on quartz wool within a vertical silica tube (30 mm inner diameter) that was later heated by an electric furnace (Fig. 1). Once the experiment was set-up, the reactor was purged with argon to remove oxygen that could oxidise the CNTs.[23] Ultra high purity (UHP) grade gases as supplied by AFROX Ltd (South Africa) were used in this study. The feedstock consisted of a mixture of CO_2 (99.99% minimum purity) and hydrogen (H_2) (99.99% minimum purity). Growth experiments were conducted at temperatures ranging from 740–850 °C.

Transmission electron microscopy (TEM, JEOL JEM-4010) was used to characterize the surface morphology of the CNTs. The samples for the TEM observations were prepared by ultrasonically dispersing them in 5 ml methanol (for 10 minutes) and then, depositing a drop of the solution onto a lacey carbon film on a copper grid. The degree of crystallinity and type of CNTs were evaluated by Raman spectroscopy using the standard 514.5 nm line of an argon ion laser.

Kinetic model formulation

Several models have been suggested for the growth of CNTs using catalysts, for example, the scooter model,[24,25] metal-particle model,[26] fullerene-cap model,[27] *etc.* However, the vapour–liquid–solid (VLS) growth model is the most popular to explain the growth of CNTs using catalysts.[28] In this model, the liquid catalyst particle plays the following roles: (i) as a catalyst for the decomposition or reduction of the carbon feedstock (*e.g.*, CO, CO_2, CH_4 or alcohols), (ii) as a solvent for the carbon atoms that are released from the feedstock, and (iii) as a soft template for the nucleation and growth of the CNTs. According to the VLS growth model, the carbon feedstock is initially in the vapour phase before dissolving into the metal catalyst to form a liquid metal–carbide particle. When this particle is carbon-saturated, the solid phase CNTs begin to grow.[29] It has been generally assumed that carbon diffusion through the catalyst bulk or over the catalyst nanoparticle is the only rate limiting step in the CNT growth process.[30] However, CNT growth rate in CVD can be limited by several other steps such as diffusion and mass transfer in the gas phase, surface reactions on the catalyst,

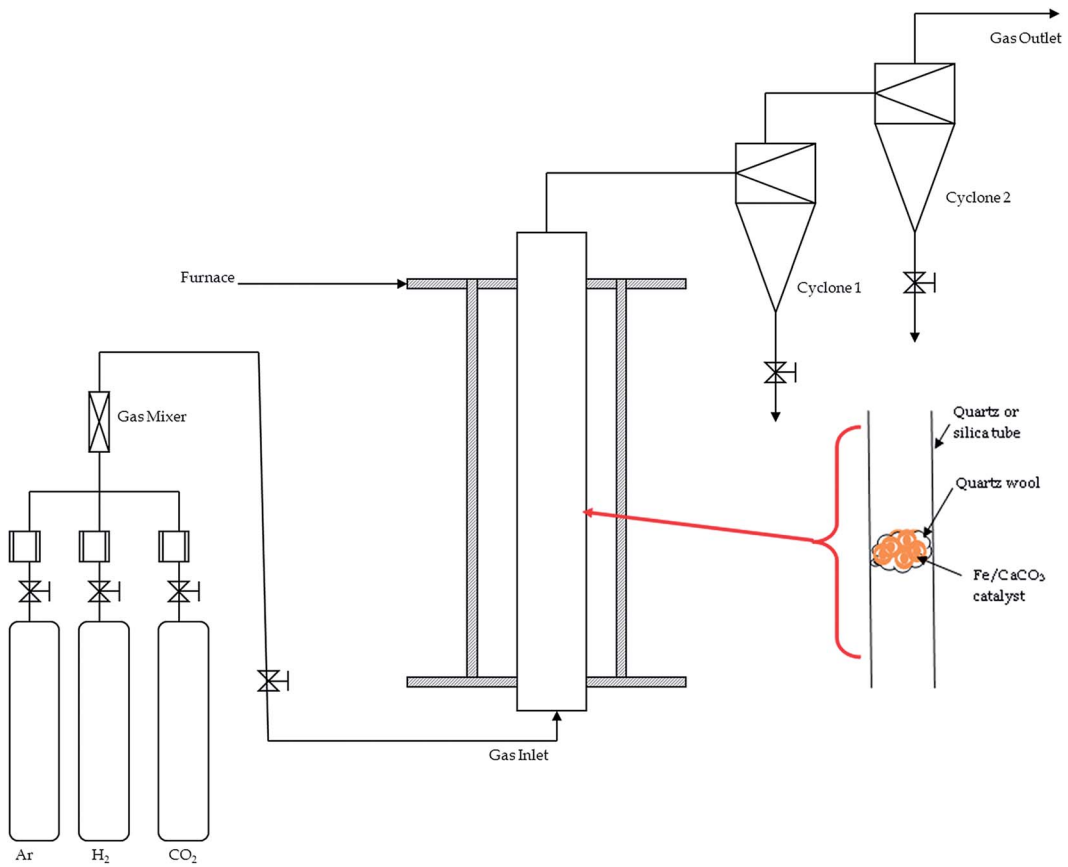

Fig. 1 Schematic of the reactor.

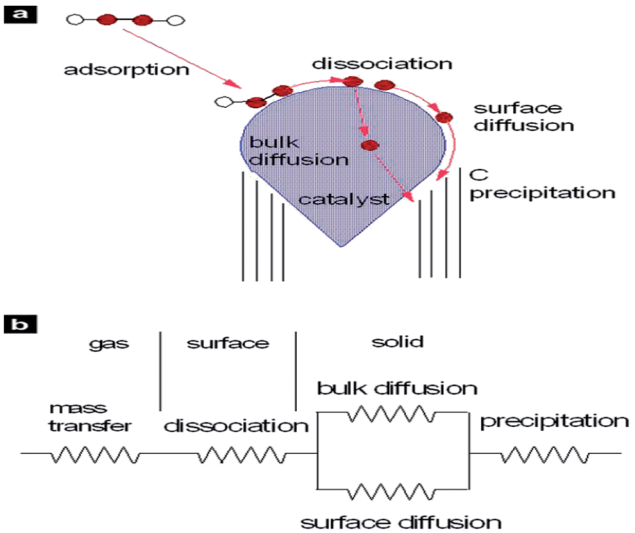

Fig. 2 (a) Schematic of the CNT growth process, (b) schematic of possible rate-limiting processes. Reproduced with permission from ref. 30.

etc., as shown schematically[30,31] in Fig. 2. Furthermore, the growth rate may also be dependent on many other factors including the gas phase decomposition reactions. Therefore, in order to understand the chemical mechanism that takes place during CNT growth from CO_2, the thermal decomposition of CO_2 should also be analysed and fully understood. The understanding of the thermal and kinetic aspects of gas phase decomposition reactions is critical in many fundamental and applied fields, for example, environmental sciences, combustion and explosions, catalysis, and planetary sciences.[32] However, gas phase decomposition can be extremely complex due to a large number of variables, a variety of possible intermediates, and an overlap in thermal decomposition traces. Nevertheless, calculations intended to provide an interpretation of the experiments are often of little help if they ignore the kinetics of the decomposition process.[32] Therefore, decomposition or reduction of CO_2 into the required chemical species is considered to be an important step here for incorporation into the rate equation for the production of CNTs.

For several decades, the decomposition or reduction of CO_2 over metal substrates has been studied for industrial processes and pollution control.[33–35] The catalysed or un-catalysed thermal splitting of CO_2 involves the following overall reaction:[36]

$$CO_2 \rightarrow C + O_2 \quad (1)$$

However, the initial stage in the splitting of CO_2 produces carbon monoxide (CO) and oxygen[18,36,37] as shown in reaction (2).

$$2CO_2 \rightarrow 2CO + O_2 \quad (2)$$

After reaction (2), the two reactions which merit consideration as possible means for the complete splitting process are either *via* the Boudouard reaction which involves the disproportionation of CO to carbon and CO_2 (see reaction (3)) or direct splitting of CO to carbon and oxygen as given by reaction (4).

$$2CO \rightarrow C + CO_2 \quad (3)$$

$$CO \rightarrow C + 1/2O_2 \quad (4)$$

However, the reaction represented by eqn (4) can be ruled out because it is only likely to occur at extremely high temperatures.[36] Therefore, reaction (3) is the only one considered here, and this reaction on iron catalyst has long been known to produce filamentous carbon;[38] such filaments with a tubular graphic structure later came to be called CNTs.[39] In fact, CO has now become one of the common carbon sources for the production of CNTs[40–43] due to the reasonable temperature range for CO disproportionation and the good CNT yield.[44] Modelling of CNT production from CO is rare except for the numerical simulations of a HiPco floating catalyst CVD reactor.[40,45]

There are a number of possible elementary reaction processes occurring before the production of CNTs. Initially, CO_2 adsorbs on the catalyst surface,

$$CO_{2(gas)} \leftrightarrow CO_{2(ads)} \quad (5)$$

and then dissociates reversibly into two adsorbed fragments of CO and oxygen as shown in reaction (6):

$$CO_{2(ads)} \leftrightarrow CO_{(ads)} + O_{(ads)} \quad (6)$$

The reaction rates for reaction (6) can be calculated for the forward and reverse reactions as,

$$R_{forward} = k_1[CO_{2(ads)}] \quad (7)$$

$$R_{reverse} = k_{-1}[CO_{(ads)}][O_{(ads)}] \quad (8)$$

The adsorbed CO in reaction (6) first dissociates into carbon and oxygen, and then, the adsorbed oxygen reacts with the undissociated CO to form surface or adsorbed[44] CO_2 which desorbs to gaseous CO_2 as shown in reactions (9), (10), and (11), respectively.

$$CO_{(ads)} \leftrightarrow C_{(ads)} + O_{(ads)} \quad (9)$$

$$CO_{(ads)} + O_{(ads)} \leftrightarrow CO_{2(ads)} \quad (10)$$

$$CO_{2(ads)} \leftrightarrow CO_{2(gas)} \quad (11)$$

In order to obtain the rate equation for the Boudouard reaction, reactions (9) and (10) are first combined as overall reaction (12),

$$2CO_{(ads)} \leftrightarrow C_{(ads)} + CO_{2(ads)} \quad (12)$$

The rate constants for the forward and reverse reactions (12) of the equilibrium are given as k_2 and k_{-2} in eqn (13) and (14), respectively,

$$R_{forward} = k_2[CO_{(ads)}]^2 \quad (13)$$

$$R_{reverse} = k_{-2}[C_{(ads)}][CO_{2(ads)}] \quad (14)$$

As shown in Fig. 2, the carbon species produced in reaction (12) diffuse into or on the surface of the catalyst particles,

nucleate and segregate to the surface forming the graphene networks of CNTs,

$$C_{(ads)} \rightarrow CNT \quad (15)$$

which is given by the following CNT growth rate:

$$\frac{d[CNT]}{dt} = k_3[C_{(ads)}] \quad (16)$$

In eqn (16), k_3 is the rate constant proportional to the diffusion coefficient (or rate) of carbons in the metal catalyst nanoparticles.[46] If the rates of formation of the intermediate products and their decay back into reactants were much faster than the rate of formation of CNTs ($k_1 \gg k_3$; $k_2 \gg k_3$), then the rate-determining step of CNT growth would be the reaction (15). In other words, reactions (5), (6), (9) and (10) are fast reactions followed by a slower reaction of carbon diffusing through (or on the) solid catalyst and precipitating to form the nanotube. Since it is assumed that the reactants are in equilibrium with the intermediate products, the equilibrium constants, K_1 and K_2, are then defined as follows:

$$K_1 = \frac{k_1}{k_{-1}} = \frac{[CO_{(ads)}][O_{(ad)}]}{[CO_{2(ad)}]} \quad (17)$$

$$K_2 = \frac{k_2}{k_{-2}} = \frac{[C_{(ads)}][CO_{2(ad)}]}{[CO_{(ad)}]^2} \quad (18)$$

Therefore, the growth rate of CNTs is given as follows:

$$\frac{d[CNT]}{dt} = k_3[C_{(ads)}] = K[CO_2] \quad (19)$$

where K is the rate constant that incorporates [O], k_3, K_1, and K_2. The overall rate as shown in eqn (19) is proportional to the concentration of adsorbed carbon atoms, $[C_{(ads)}]$, or it is proportional to the concentration of CO_2, $[CO_2]$. Eqn (19) is a simple kinetic model equation for predicting the rate of CNT production from CO_2. The rate constant, K, is proportional to the diffusion coefficient of carbon.[46] Therefore, in this study, the activation energy (E_a) of the rate constant was taken as the diffusion energy of carbon[47,48] into the bulk iron metal (γ-Fe), *i.e.* 35 kcal mol^{-1}.

H_2 was used in this work together with CO_2 as mentioned in the materials and methods section. Nasibulin and colleagues have already demonstrated the important role of H_2 in the CVD process.[43] However, the following needs to be noted: H_2 is believed to prevent the oxidation of the nanosized catalyst iron particles, thus maintaining the catalyst in their reduced state.[43,44,49] In fact, Moisala *et al.*[50] thermodynamically showed that only non-oxide metal particles behave as catalysts in the CNT formation, thus metal oxide particles must be reduced. In addition, H_2 limits or alleviates the carbon poisoning of the metal catalysts.[51] It has also been reported that adsorbed H_2 on the catalyst surface catalyses the disproportionation[52] of CO. Though not related to this study, H_2 reduces the rate of dehydrogenation of the CH_x intermediates which are responsible for soot formation.[53] Finally, at the studied furnace temperature, H_2 can provide additional carbon atoms for the CNT synthesis from its reaction with CO_2 under the temperature conditions of this study as shown in eqn (20) below.[18,44]

$$CO_2 + 2H_2 \leftrightarrow 2H_2O + C \quad (20)$$

However, the reaction with CNTs and hydrogen, as given by reaction (21),

$$2C + 4H_2 \leftrightarrow 2CH_4 \quad (21)$$

also occurs in the reactor, where CNTs are reduced to methane.[43] This reaction counters the effect of CNT produced due to the presence of H_2 (eqn (20)). Therefore, it is assumed here that only the first, second, and third roles of H_2 above are applicable, *i.e.*, H_2 does not need to be included in the simple kinetic eqn (19). Finally, catalyst deactivation is not considered in this simple model formulation and would be considered in future improvements.

Results and discussion

Identification of CNTs

The TEM images in Fig. 3 confirms that the deposited carbons are CNTs, produced at temperatures 750, 800 and 840 °C. The filamentous carbon possesses hollow cores without any bamboo-like closures and the diameter distribution of the as-produced CNTs is rather uniform with an average diameter less than 100 nm. Fig. 4 is the Raman spectra of the as-grown CNTs shown also for growth temperatures of 750, 800 and 840 °C. The basis for the Raman spectra revolves around the assignment of the G-band (graphitic, ~1580 cm^{-1}) to crystalline graphite and any other bands, called D-bands (disorder, varies from 1100 to 1500 cm^{-1}) to any type of structural disorder in the graphitic structure.[54] However, the other band that is characteristic only for single-walled CNTs called radial breathing mode (RBM) lie in the region[55] of 100–400 cm^{-1}. Fig. 4 shows two significant peaks at ~1358 cm^{-1} and ~1582 cm^{-1}, representing the D-band and G-band, respectively. As stated already, the G-band represents the graphitisation degree of the nanotube structure while the D-band describes the degree of structural defects including amorphous (non-graphitic) carbon adhered on the nanotube structure.[56,57] The absence of the RBM in the Raman spectra implies that the CNTs produced are multi-walled.

The I_D/I_G ratio, which shows the relative intensity of the D- and G-bands of a Raman spectrum and an indicator of the degree of graphitization and crystallinity,[57,58] has ratios of 0.99, 1.08 and 1.02 for temperatures of 750, 800 and 840 °C respectively. These values suggest that the as-produced CNTs exhibit a remarkable crystallinity as the temperature increases, implying that the raw CNTs have smoother carbon surfaces and less structural defects. These results agree with the TEM images in Fig. 3. In general, the purity of CNTs produced in this study is high and the higher purity of CNTs from CO_2 relative to those produced from gaseous hydrocarbons was also reported by Xu and Huang.[18]

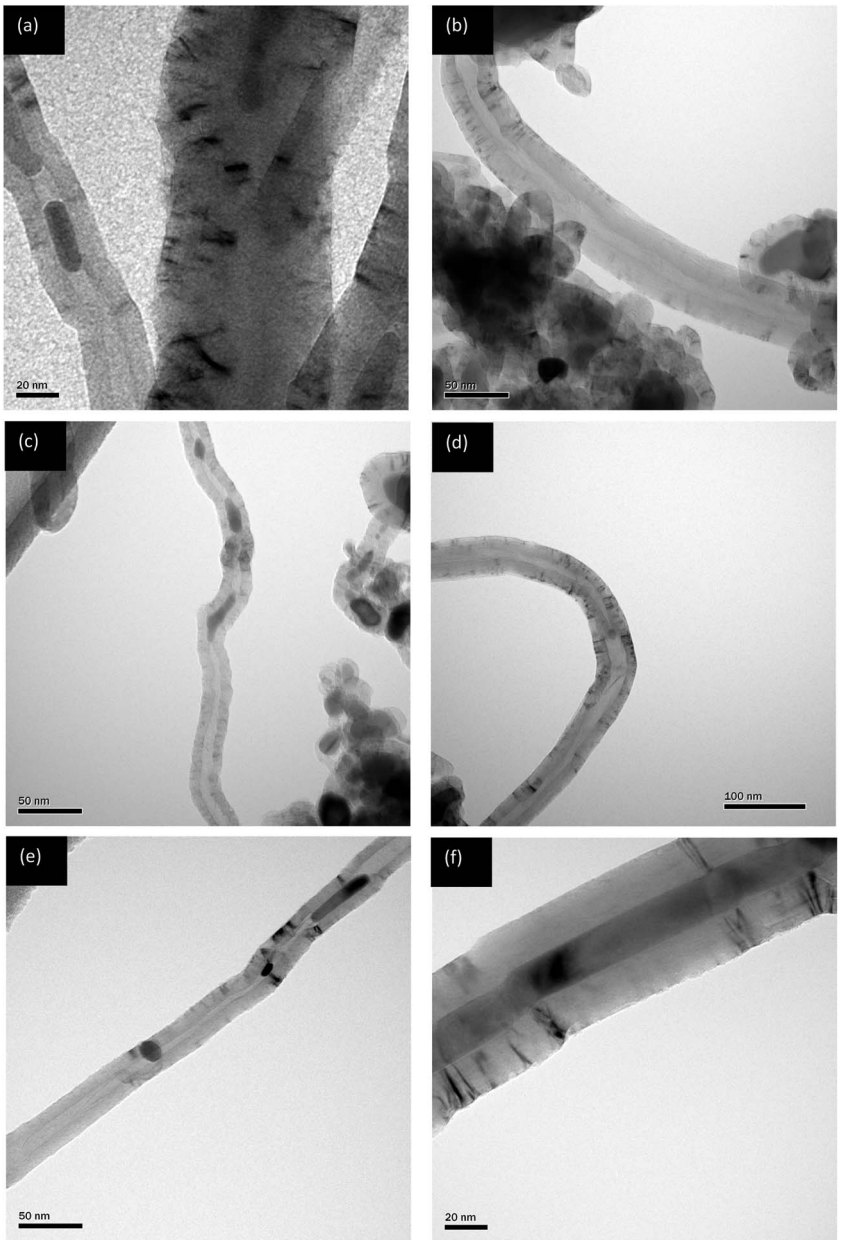

Fig. 3 TEM images of multi-walled CNTs at (a), (b) 750 °C, (c), (d) 800 °C, (e), (f) 840 °C.

Comparison of kinetic model with experimental data

The derived kinetic model can be used to calculate the amount or yield of CNTs for a given volumetric flow rate (or concentration) of CO_2. A comparison of the simulated results and the experimental as well as the general effects (not based on the model, but on the actual observations) of other parameters on the production of CNTs are discussed below.

Effect of carbon dioxide concentration. The experimental production rates of CNTs at different concentrations of CO_2 at a temperature of 800 °C are compared with the simulated results in Fig. 5. The CNT production is the highest at 800 °C as shown later in Fig. 6. Fig. 5 shows that the production of CNTs initially increases with the concentration of CO_2 up to a concentration of about 5000 ppm. Thereafter, the gradient in the plot decreases with an increase in CO_2 concentration. This means that the rate of production per unit quantity of CO_2 reduces as reported previously by others.[59–61] These studies also found that as carbon concentration in the feedstock increases, the CNT yield decreases significantly. The rate of formation of adsorbed surface carbon exceeds the diffusion rate at higher carbon concentrations, leading to the formation of monolayer or multiple layers of carbon on the catalyst particles. This phenomenon stops further surface reactions resulting in the confinement of the catalyst. In the case of lower carbon concentration in the gas phase, the rate of formation of adsorbed surface carbon is lower than or equal to the rate of diffusion and precipitation of carbon in the form of CNTs, resulting in a continuous production process.[61]

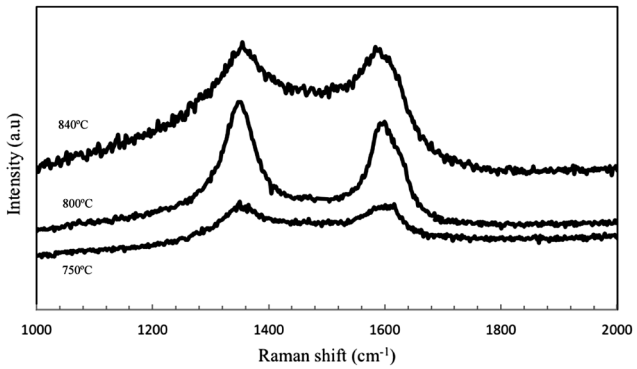

Fig. 4 Raman spectrum of the CNTs produced at 750, 800 and 840 °C.

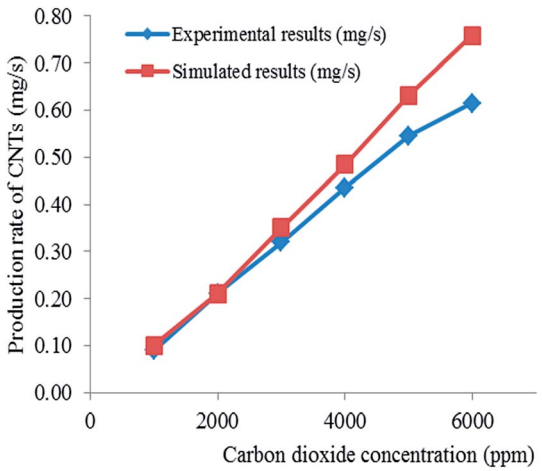

Fig. 5 The experimental and simulated production rates of carbon nanotubes at 800 °C.

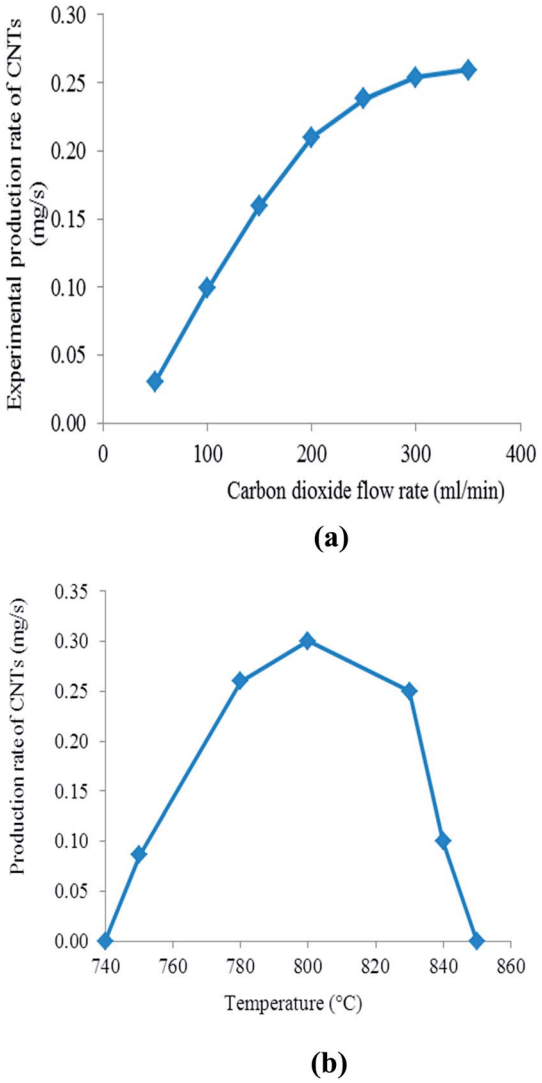

Fig. 6 (a) Effect of volumetric flow rate on the production rate of carbon nanotubes and (b) effect of temperature on the production rate of carbon nanotubes at 400 ml min^{-1} carbon dioxide.

Effect of volumetric flow rate of carbon dioxide. Fig. 6(a) shows the effect of the volumetric flow rate of CO_2 on CNT production rate, for a reactor temperature of 800 °C after a reaction time of 45 minutes. Initially, an increase in flow rate increases the rate of CNT production. However, at higher flow rates the rate of production of CNT is reduced. This is because a higher volumetric flow rate reduces the residence time for the reaction, leading to the production of lower number of carbon atoms during the reaction. These results agree with the findings by Singh *et al.*[62] and Toussi *et al.*[63] showing that higher flow rate of the carbon source led to the production of fewer CNTs. In contrast, Vallés *et al.*[64] found that higher carbon feedstock supply rates led to an increased CNT yield.

Effect of reactor temperature. Temperature is a very important parameter that affects both the decomposition of CO_2 and the disproportionation of CO. The effect of temperature on the CNT production rate is shown in Fig. 6(b) which indicates that growth only occurs between 750 and 840 °C. Initially, the rate of production increases with an increase in temperature up to about 800 °C, and then, it reduces drastically. An increase in temperature in the first region implies that there is enough energy to initiate the decomposition of CO_2 leading to the formation of CNTs from the CO disproportionation reaction. However, at higher temperatures the production rates of CNTs decreases until finally ceasing at approximately 850 °C. These results may be explained from CO_2 decomposition, Boudouard reaction requirements, and the kinetics of carbon diffusion as discussed below.

The CO disproportionation reaction (eqn (3) or (12)) has two main limitations, namely: (1) the reaction is limited kinetically at lower temperatures, and (2) it is limited thermodynamically at higher temperatures.[43] Previous studies have shown that kinetic and thermodynamic factors limit the effective CO disproportionation reaction to a temperature range of 520–800 °C at atmospheric pressure.[50] Equilibrium favours the right side[65] at temperatures below 700 °C. The observations by Moisala *et al.*[50] and Boehm[65] agree with the results of this study which show an increase in CNT production for temperatures lower than about 800 °C. However, attainment of equilibrium is possible only in the presence of catalysts, mainly iron, cobalt, and nickel. Even then, temperatures in excess of 400 °C are

needed for measurable reaction rates, with maximum rates observed[65] around 550 °C. Furthermore, previous studies have also shown that although the conversion of CO may be fast at lower temperatures, the CNT yield is very low.[66] This is because the plentiful amount of carbon that forms on the catalyst surface is not able to be transferred away in time due to the relatively low rate of carbon diffusion in the bulk of the metal catalyst particles at low temperatures, and thus, blocks the active catalyst surface leading to a decrease in activity.[66]

In summary, CO_2 decomposition is an endothermic reaction with CO formation being favoured at higher temperatures. In contrast, CO disproportionation is an exothermic reaction, such that both the CO conversion and carbon formation decline as the reaction temperature is increased. In addition, at higher temperatures, CO_2 acting as a mild oxidising agent can react with the graphitic layers of the CNTs, leading to the erosion of CNTs and thus, a low yield is achieved.[67] There are no oxidation reactions for CNTs at lower temperatures.[68]

Since the Boudouard reaction is an exothermic reaction limited by equilibrium at the high temperatures needed to activate CO on the catalyst, it has been found that high CO partial pressures are needed in order to counter the effect of temperature and drive the reaction in the forward direction.[43,69,70] Therefore, high pressure results in both the enhancement of the reaction rate due to an increase in the amount of reagent and in the widening of the temperature range for CNT production.[43]

Importance of further kinetic model development for large-scale CNT synthesis

Mass production of CNTs continues to be a challenge and though the literature has been vast and growing, kinetic models are scarce. Table 1 outlines the limited kinetic models available and the limited number of studies has an impact on our understanding and the consequent slow progress. The use of pure gases (hydrocarbons or otherwise) as feedstock is very expensive as they are limited in supply. Moreover, most organic gases are toxic and difficult to store and transport. The precursor materials for bulk production of CNTs should be economically attractive, available in plentiful supply and easy to pyrolyze.[7] Studies have shown that CNTs can be successfully produced from liquefied petroleum gas,[75] natural gas,[76] coal gas[77,78] and directly from coal.[79] However, more experimental work is needed to improve the yield and quality of CNTs produced from these 'impure' carbon sources. A major challenge in using these impure sources is that complete study of the species present in the gas phase at high temperature is difficult to achieve, as decomposition of the carbon precursor involves many steps. Additionally, the recombination and reactivity of the initial species make it difficult to know which species are in fact the true gas phase intermediates that actively take part in the growth of CNTs.[80] As a result, the possible synergic effect of gaseous species in coal gas that results in CNT synthesis is unclear.[77,78] In order to fulfill this requirement, the kinetic model (eqn (19)) developed for CNT production from CO_2 needs to be modified to make the provisional first steps in understanding these possible effects.

Conclusions

The combination of the potential decomposition mechanisms of CO_2 and carbon diffusion was utilised to formulate a simple kinetic model for the production of CNTs. The results illustrate the importance of including the thermal decomposition step. There is no well-known kinetic model to date for the production of CNTs from CO_2 and the kinetic model derived here was used

Table 1 Kinetic models for CNT synthesis

Carbon Source	Catalyst	Proposed model for CNT production	Ref.
Carbon monoxide (CO)	$Fe(CO)_5$	$d[Fe_mC_{NT}]/dt = \beta k_3[Fe_mCO][CO]$ whereby : $\beta = \frac{1}{(2n_{NT}-1)}$	40,45
Acetylene (C_2H_2)	Iron supported (Fe/silica)	$r_C(t) = r_{C_0}[a_s + k_G\alpha\exp(-k_Gt) - k_B\beta\exp(-k_Bt)]$ whereby : $\alpha = \frac{k_B(1-a_S)}{k_G(k_B-k_G)}$, $\beta = \frac{(k_B-k_Ga_S)}{k_B(k_B-k_G)}$	71
Acetylene (C_2H_2)	Ferrocene	$\frac{d[CNT]}{dt} = k_d[C]_{excess} = k_dK[C]_{free}[C]_{sat} = (K[C]_{free})k_d[C]_{sat} = Ak_d[C]_{sat}$	46
Acetylene (C_2H_2)	Ni- and Co-supported $CaCO_3$	$R_a = \frac{1}{w_{CAT}}\frac{dw_{CNT}}{dt} = A\exp\left(-\frac{E}{RT}\right)(P_{C_2H_2})^n$	72,73
Ethylene (C_2H_4)	Fe/Al_2O_3	$\left(\frac{dX_1}{dt}\right)_{t=0} = 69.97(\%_{Fe}m_{CAT})^{0.28} \times \exp\left(-\frac{29\,000}{RT}\right)(y_{C_2H_4})^{0.75}$	74
Carbon dioxide (CO_2)	Fe-supported $CaCO_3$	$\frac{d[CNT]}{dt} = k_3[C_{(ads)}] = K[CO_2]$	This study

to calculate the amount of CNTs at various concentrations of CO_2. The experimentally measured production rate data fits the simple rate equation very well at low CO_2 concentrations. The analysis here can be extended to other carbon sources used in the production of CNTs. The influence of CO_2 flow rate was also studied. Just like concentration, very high flow rates adversely affect the CNT growth rates indicating the importance of controlling the concentration and flow rate of the carbon source. The results also show that the temperature plays an important role in the synthesis of CNTs from CO_2: when the temperature is lower than 750 °C or above 840 °C, no CNTs are formed and the optimum growth temperature is about 800 °C.

Acknowledgements

The authors wish to thank Dr Lubinda F. Walubita of TTI – The Texas A&M University System (USA) for his insightful technical comments on the paper. The financial support from the National Research Foundation (NRF) under South Africa NRF Focus Area, NRF Nanotechnology flagship programme, DST/NRF Centre of Excellence and University of the Witwatersrand Staff Bursary is gratefully acknowledged.

References

1 M. Aresta, *Stud. Surf. Sci. Catal.*, 1998, **114**, 65–76.
2 Q. W. Chen and D. W. Bahnemann, *J. Am. Chem. Soc.*, 2000, **122**, 970–971.
3 G. A. Olah, A. Goeppert and G. K. S. Prakash, *J. Org. Chem.*, 2009, **74**, 487–498.
4 F. T. Zangeneh, S. Sahebdelfar and M. T. Ravanchi, *J. Nat. Gas Chem.*, 2011, **20**, 219–231.
5 G. S. Simate, S. E. Iyuke, S. Ndlovu, C. S. Yah and L. F. Walubita, *J. Nat. Gas Chem.*, 2010, **19**, 453–460.
6 M. Meyyappan, *Carbon Nanotubes: Science and Applications*, Boca Raton, FL, CRC Press, 2004.
7 K. Dasgupta, J. B. Joshi and S. Banerjee, *Chem. Eng. J.*, 2011, **171**, 841–869.
8 S. E. Iyuke and A. B. M. Danna, *Microporous Mesoporous Mater.*, 2005, **84**, 338–342.
9 A. S. Afolabi, A. S. Abdulkareem and S. E. Iyuke, *J. Exp. Nanosci.*, 2007, **2**, 269–277.
10 S. E. Iyuke, T. A. Mamvura, K. Liu, V. Sibanda, M. Meyyappan and V. K. Varadan, *Nanotechnology*, 2009, **20**, 375602–375611.
11 N. M. Mohamed and L. M. Kou, *J. Appl. Sci.*, 2011, **11**, 1341–1345.
12 J. M. Ngoy, S. E. Iyuke, W. E. Neuse and C. S. Yah, *J. Appl. Sci.*, 2011, **11**, 2700–2711.
13 L. Fekri, A. Jafari, S. Fekri, A. Shafikhani, M. Vesaghi and G. Behzadi, *J. Appl. Sci.*, 2010, **10**, 716–723.
14 M. Khavarian, S. P. Chai, S. H. Tan and A. R. Mohamed, *J. Appl. Sci.*, 2011, **11**, 2382–2387.
15 E. Mora, T. Tokune and A. R. Harutyunyan, *Carbon*, 2007, **45**, 971–977.
16 A. S. Anisimov, A. G. Nasibulin, H. Jiang, P. Launois, J. Cambedouzou and S. D. Shandakov, *Carbon*, 2010, **48**, 380–388.
17 L. Ci, Y. Li, B. Wei, J. Liang, C. Xu and D. Wu, *Carbon*, 2000, **38**, 1933–1937.
18 X.-J. Xu and S.-M. Huang, *Mater. Lett.*, 2007, **61**, 4235–4237.
19 S. D. Mhlanga, Synthesis and study of carbon nanotubes and carbon spheres, PhD thesis, Johannesburg, University of the Witwatersrand, 2009.
20 C. H. See and A. T. Harris, *AIChE J.*, 2008, **54**, 657–664.
21 Z. Li, E. Dervishi, Y. Xu, V. Saini and M. Mahmood, *Catal. Lett.*, 2009, **131**, 356–363.
22 C. S. Yah, S. E. Iyuke, G. S. Simate, E. I. Unuabonah, G. Bathgate and G. Matthews, *J. Mater. Res.*, 2011, **26**, 640–644.
23 C. S. Yah, G. S. Simate, K. Moothi, S. K. Maphutha and S. E. Iyuke, *Trends Appl. Sci. Res.*, 2011, **6**, 1270–1279.
24 A. Thess, R. Lee, P. Nikolaev, H. Dai, P. Petit, J. Robert and C. Xu, *Science*, 1996, **273**, 483–487.
25 Y. H. Lee, S. G. Kim and D. Tomanek, *Phys. Rev. Lett.*, 1997, **78**, 2393–2396.
26 M. Yudasaka, R. Yamada, N. Sensui, T. Wilkins, T. Ichihashi and S. Iijima, *J. Phys. Chem. B*, 1999, **103**, 6224–6229.
27 H. Kataura, Y. Kumazawa, Y. Maniwa, Y. Ohtsuka, R. Sen and S. Suzuki, *Carbon*, 2000, **38**, 1691–1697.
28 Y. Saito, *Carbon*, 1995, **33**, 979–988.
29 K. Raji, S. Thomas and C. B. Sobhan, *Appl. Surf. Sci.*, 2011, **257**, 10562–10570.
30 C. T. Wirth, C. Zhang, G. Zhong, S. Hofmann and J. Robertson, *ACS Nano*, 2009, **3**, 3560–3566.
31 S. Hofmann, G. Csanyi, A. C. Ferrari, M. C. Payne and J. Robertson, *Phys. Rev. Lett.*, 2005, **95**, 036101.
32 O. Sharia and M. M. Kuklja, *J. Phys. Chem. A*, 2010, **114**, 12656–12661.
33 R. G. Copperthwaite, P. R. Davies, M. A. Morris, M. W. Roberts and R. A. Ryder, *Catal. Lett.*, 1988, **1**, 11–19.
34 H. Kato, T. Kodama, M. Tsuji, Y. Tamaura and S. C. Chang, *J. Mater. Sci.*, 1994, **29**, 5689–5692.
35 Z. Chun-lei, L. Zhi-qiang, W. Tong-hao, Y. Hong-mao, J. Yu-zi and P. Shao-yi, *Mater. Chem. Phys.*, 1996, **44**, 194–198.
36 S. Rayne, Thermal carbon dioxide splitting: A summary of the peer-reviewed scientific literature, *Nature Precedings*, 2008, DOI: 10.1038/npre.2008.1741.2.
37 H. C. Shin, S. C. Choi, K. D. Jung and S. H. Han, *Chem. Mater.*, 2001, **13**, 1238–1242.
38 M. Monthioux and V. L. Kuznetsov, *Carbon*, 2006, **44**, 1621–1623.
39 S. Iijima, *Nature*, 1991, **354**, 56–58.
40 C. Dateo, T. Gokcen and M. Meyyappan, *J. Nanosci. Nanotechnol.*, 2002, **2**, 523–534.
41 A. G. Nasibulin, A. Moisala, D. P. Brown and E. I. Kauppinen, *Carbon*, 2003, **41**, 2711–2724.
42 A. Moisala, A. G. Nasibulin, D. P. Brown, H. Jiang, L. Khriachtchev and E. I. Kauppinen, *Chem. Eng. Sci.*, 2006, **61**, 4393–4402.
43 A. G. Nasibulin, P. Queipo, S. D. Shandakov, D. P. Brown, H. Jiang and P. V. Pikhitsa, *J. Nanosci. Nanotechnol.*, 2006, **6**, 1233–1246.
44 G. Lanzani, A. G. Nasibulin, K. Laasonen and E. I. Kauppinen, *Nano Res.*, 2009, **2**, 660–670.

45 T. Gokcen, C. Dateo and M. Meyyappan, *J. Nanosci. Nanotechnol.*, 2002, **2**, 535–544.
46 K. E. Kim, K. J. Kim, W. S. Jung, S. Y. Bae, J. Park and J. Choi, *Chem. Phys. Lett.*, 2005, **401**, 459–464.
47 R. T. K. Baker, *Carbon*, 1989, **27**, 315–323.
48 E. A. Brandes and G. B. Book, *Smithells Metals Reference Book*, London, Butterworth-Heinemann Limited, 7th edn, 1992.
49 M. C. Bahome, L. L. Jewell, D. Hildebrandt, D. Glasser and N. J. Coville, *Appl. Catal., A*, 2005, **287**, 60–67.
50 A. Moisala, A. G. Nasibulin and E. I. Kauppinen, *J. Phys.: Condens. Matter*, 2003, **15**, S3011–S3035.
51 M. S. Kim, N. M. Rodriguez and R. T. K. Baker, *J. Catal.*, 1991, **131**, 60–73.
52 B. Zheng, C. Lu, G. Gu, A. Makarovski, G. Finkelstein and J. Liu, *Nano Lett.*, 2002, **2**, 895–898.
53 P. T. A. Reilly and W. B. Whitten, *Carbon*, 2006, **44**, 1653–1660.
54 S. Potgieter-Vermaak, N. Maledi, N. Wagner, J. H. P. van Heerden, R. van Grieken and J. H. J. Potgieter, *Raman Spectrosc.*, 2011, **42**, 123–129.
55 S. Osswald, M. Havel and Y. J. Gogotsi, *Raman Spectrosc.*, 2007, **38**, 728–736.
56 S. P. Patole, P. S. Alegaonkar, J. H. Lee and J. B. Yoo, *Europhys. Lett.*, 2008, **81**, 1–6.
57 K. Y. Lee, W. M. Yeoha, S. P. Chaib, S. Ichikawac and A. R. Mohameda, *Fullerenes, Nanotubes, Carbon Nanostruct.*, 2010, **18**, 273–284.
58 T. Tsoufis, P. Xidas, L. Jankovic, D. Gournis, A. Saranti and T. Bakas, *Diamond Relat. Mater.*, 2007, **16**, 155–160.
59 R. Andrews, D. Jacques, A. M. Rao, F. Derbyshire, D. Qian and X. Fan, *Chem. Phys. Lett.*, 1999, **303**, 467–474.
60 X. Y. Li, B. C. Huang and N. J. Coville, *Fullerenes, Nanotubes, Carbon Nanostruct.*, 2002, **10**, 339–352.
61 R. M. M. Abbaslou, J. Soltan and A. K. Dalai, *Appl. Catal., A*, 2010, **372**, 147–152.
62 C. Singh, M. S. P. Shaffer and A. H. Windle, *Carbon*, 2003, **41**, 359–368.
63 S. M. Toussi, A. Fakhru'l-Razi, A. L. Chuah and A. R. Suraya, *Mater. Sci. Eng.*, 2011, **17**, 012003.
64 C. Vallés, M. Pérez-Mendoza, W. K. Maser, M. T. Martínez, L. Alvarez and J. L. Sauvajol, *Carbon*, 2009, **47**, 998–1004.
65 H. P. Boehm, *Carbon*, 1973, **11**, 583–536.
66 P. Chen, H. B. Zhang, G. D. Lin, Q. Hong and K. R. Tsai, *Carbon*, 1997, **35**, 1495–1501.
67 S. C. Tsang, P. J. F. Harris and M. L. H. Green, *Nature*, 1993, **362**, 520–522.
68 Z. Lou, C. Chen, Q. Chen and J. Gao, *Carbon*, 2005, **43**, 1104–1108.
69 P. Nikolaev, M. J. Bronikowski, R. K. Bradley, F. Rohmund, D. T. Colbert and K. A. Smith, *Chem. Phys. Lett.*, 1999, **313**, 91–97.
70 D. E. Resasco, W. E. Alvarez, F. Pompeo, L. Balzano, J. E. Herrera and B. Kitiyanan, *J. Nanopart. Res.*, 2002, **4**, 131–136.
71 M. P. Cabero, E. Romeo, C. Royo, A. Monzon, A. G. Ruiz and I. Rodríguez-Ramos, *J. Catal.*, 2004, **224**, 197–205.
72 C. T. Hsieh, Y. T. Lin, J. Y. Lin and J. L. Wei, *Chem. Phys.*, 2009, **114**, 702–708.
73 C. T. Hsieh, Y. T. Lin, W. Y. Chen and J. L. Wei, *Powder Technol.*, 2009, **192**, 16–22.
74 R. Philippe, P. Serp, P. Kalck, Y. Kihn, S. Borde're and D. Plee, *AIChE J.*, 2009, **55**, 450–464.
75 W. Qian, H. Yu, F. Wei, Q. Zhang and Z. Wang, *Carbon*, 2002, **40**, 2961–2973.
76 R. Bonadiman, M. D. Lima, M. J. de Andrade and C. P. Bergmann, *J. Mater. Sci.*, 2006, **41**, 7288–7295.
77 J. Qiu, Y. An, Z. Zhao, Y. Li and Y. Zhou, *Fuel Process. Technol.*, 2004, **85**, 913–920.
78 J. Qiu, Q. Li, Z. Wang, Y. Sun and H. Zhang, *Carbon*, 2006, **44**, 2565–2568.
79 K. Moothi, S. Iyuke, M. Meyyappan and R. Falcon, *Carbon*, 2012, **50**, 2679–2690.
80 A. Shaikjee and N. J. Coville, *Carbon*, 2012, **50**, 3376–3398.